ISSN 1063-7729, Astronomy Reports, 2019, Vol. 63, No. 1, pp. 49–65. © Pleiades Publishing, Ltd., 2019.
Russian Text © L.N. Vol'vach, A.E. Vol'vach, M.G. Larionov, G.C. MacLeod, S.P. van den Heever, P. Wolak, M. Olech, A.V. Ipatov, D.V. Ivanov, A.G. Mikhailov, A.E. Mel'nikov, K. Menten, A. Belloche, A. Weiss, P. Mazumdar, F. Schuller, 2019, published in Astronomicheskii Zhurnal, 2019, Vol. 96, No. 1, pp. 51–69.

# A Giant Water Maser Flare in the Galactic Source IRAS 18316-0602

**L. N. Vol'vach[1*], A. E. Vol'vach[1,2], M. G. Larionov[3], G. C. MacLeod[4], S. P. van den Heever[4], P. Wolak[5], M. Olech[5], A. V. Ipatov[2], D. V. Ivanov[2], A. G. Mikhailov[2], A. E. Mel'nikov[2], K. Menten[6], A. Belloche[6], A. Weiss[6], P. Mazumdar[6], and F. Schuller[6,7]**

[1]*Department of Radio Astronomy and Geodynamics, Crimean Astrophysical Observatory, Katsivelli, Russia*
[2]*Institute of Applied Astronomy, Russian Academy of Sciences, St. Petersburg, 191187 Russia*
[3]*Astro Space Center, Lebedev Physical Institute, Russian Academy of Sciences, Moscow, 117997 Russia*
[4]*Hartebeesthoek Radio Astronomy Observatory, P.O.Box 443, Krugersdorp 1740, South Africa*
[5]*Torun Centre for Astronomy, Nicolaus Copernicus University, Piwnice, PL-87-148 Lysomice, Poland*
[6]*Max-Planck-Institut für Radioastronomie, Auf dem Hügel 69, D-53121 Bonn (Endenich), Germany*
[7]*Université Paris Diderot, Gif-sur-Yvette, France*

Received April 27, 2018; in final form, June 22, 2018

**Abstract**—The results of long-term monitoring of the Galactic maser source IRAS 18316-0602 (G25.65+1.05) in the water-vapor line at frequency $f = 22.235$ GHz ($6_{16}$–$5_{23}$ transitioin) carried out on the 22-m Simeiz, 26-m HartRAO, and 26-m Torun radio telescopes are reported. The source has been episodically observed on the Simeiz telescope since 2000, with more regular observations beginning in 2017. A double flare was observed beginning in September 2017 and continuing to February 2018, which was the most powerful flare registered over the entire history of observations of this object. Most of the monitoring of the flare was carried out in a daily regime. Detailed analysis of the variations of the flux density, which reached a maximum value $P \approx 1.3 \times 10^5$ Jy, have led to important scientific conclusions about possible mechanisms for the emission in this water line. The exponential growth in the flux density in this double flare testifies that it was associated with a maser that was unsaturated right up to the maximum flux densities observed. An additional argument suggesting the maser was unsaturated is the relatively moderate degree of linear polarization (≈30%), nearly half the value displayed by the Galactic kilomasers in Orion KL. The accurate distance estimate for IRAS 18316-0602 (12.5 kpc) and the flux density at the flare maximum ($\approx 1.3 \times 10^5$ Jy) makes this the most powerful Galactic kilomaser known. The double form of the flare with exponential rises in flux density rules out the possibility that the flare is the effect of directivity of a radiation beam relative to the observer. The physical nature of the flare is most likely related to internal parameters of the medium in which the maser clumps radiating in the water line are located. A rapid, exponential growth in the flux density of a kilomaser and associated exponential decays requires the presence of an explosive increase in the density of the medium and the photon flux, leading to an increase in the temperature by 10–40 K above the initial base level. A mechanism for the primary energy release in IRAS 18316-0602 is proposed, which is associated with a multiple massive star system located in a stage of evolution preceding its entry onto the main sequence. A flare in this object could initiate gravitational interaction between the central star and a massive companion at its periastron. The resulting powerful gravitational perturbation could lead to the ejection of the envelope of the central supermassive star, which gives rise to an explosive increase in the density and temperature of the associate gas–dust medium when it reaches the disk, where the maser clumps are located.

**DOI:** 10.1134/S1063772919010062

## 1. INTRODUCTION

After the discovery of the $6_{16}$–$5_{23}$ water transition in 1969, it was established that this maser emission is associated with HII regions or cool late-type stars [1].

In 1971, the first intercontinental VLBI observations were made, with the participation of the 22-m Simeiz telescope of the Crimean Astrophysical Observatory (CrAO). These were observations at the

*E-mail: volvach@meta.ua

frequency of the $6_{16}$–$5_{23}$ water-vapor maser transition, $f = 22.235$ GHz. An angular resolution of 0.1 milliarcsecond (mas) was achieved on the baseline between the 22-m Simeiz and 37-m Haystack antennas. Clusters of $H_2O$ clumps were found in Galactic objects, and a powerful flare was observed in the complex W49. The rapid flux variations testified to the very small dimensions of the emission region. This was confirmed by VLBI observations realizing the maximum possible angular resolution. The brightness temperature of the $H_2O$ emission regions reached $10^{16}$ K, which can be explained only as maser radiation [2].

In the dense envelopes of protostars, where the medium is heated by shocks, protostellar ejections, and the accretion of matter, the $H_2O$ content can comprise $10^{-4}$ of the gas density. This is four to five orders of magnitude higher than the mean abundance in the Galaxy [3–6]. Since it is vaporized at temperatures of about 100 K, water molecules become dominant in the gaseous component of protostars, on a par with CO. Water masers leave traces in star-forming regions in HII regions, indicating the appearance of new protostars.

$H_2O$ masers (the $6_{16}$–$5_{23}$ transition) were first detected in the Galactic infrared source IRAS 18316-0602 in March 1989, during a survey of objects from the IRAS Point Source Catalog selected according to specified criteria, mainly that the IR flux at 60 $\mu$m $F_{60}$ was at last 100 Jy and that the spectrum was steep between 12–60 $\mu$m. This work was carried out on the 32-m radio telescope in Medicina (Italy). Some 260 IR sources were observed, in 17% of which $H_2O$ masers were detected. Most of these maser sources were new, including the maser in IRAS 18316-0602 [7].

IRAS 18316-0602 is associated with the ultracompact HII region G25.65+1.05 [8]. IRAS 18316-0602 was obsrved in the radio continuum at 5 and 8 GHz, in order to derive information about its spectral energy distribution [9, 10]. Submillimeter observations were carried out at 450–1100 $\mu$m in 1995 [11, 12]. The CO line was detected at 2.6 mm in 1991 by McCutcheon et al. [9]. Observations of CS and $NH_3$ lines were also successfully conducted [13, 14].

Observations of IRAS 18316-0602 were carried out in the near-IR in order to search for bipolar outflows from star-forming regions [15]. Outflows from young, high-mass protostars were distinguished in the HII line, toward the central region of the IR source. A relationship between dense gas, maser sources, and a massive young star can be traced [16].

Both $H_2O$ and methanol maser emission associated with IRAS 18316-0602 was detected in 1994–1996 [17–19]. It was noted that, in spite of the fact that the maser power represents a negligible fraction of the bolometric luminosity of the gas–dust cloud ($10^{-9}$), there is a correlation between the $H_2O$ maser intensity and the luminosity of the host cloud in the far-IR (60 $\mu$m).

At the time of its discovery, the intgrated flux in the $H_2O$ line in IRAS 18316-0602 was $F_\nu \approx 1000$ Jy. Our observations indicate that the flux falls to as low as 10 Jy at times.

In our current study, we present new monitoring data for IRAS 18316-0602 in the $H_2O$ line carried out on the indicated radio telescopes, mainly in the period from September 2017 through February 2018. A giant double superflare in the $H_2O$ line with a record flux level occurred during this interval. As a rule, observations were obtained in a daily regime, near the culmination of the source in order to reduce the influence of the atmosphere.

## 2. OBSERVING METHOD AND DATA REDUCTIONS

A modernized spectropolarimetric radiometer with a parallel-type Fourier spectrum analyzer was used to receive and record the source signals in the water line on the 22-m CrAO telescope. This analyzer had 512 and/or 2048 channels and a resolution of 8 and/or 2 kHz (105 and/or 26 m/s in radial velocity in the $H_2O$) [20]. The spectral data obtained were corrected for atmospheric absorption and variation in the effective area of the radio telescope as a function of elevation.

The receiver bandwidth was 4 MHz when the Mark-5B+ recording system was used. The software used was written in the CrAO Radio Astronomy Department. The system noise temperature $T_{sys}$ and atmospheric absorption were determined using a calibration step, atmospheric cuts, and temperature differences for the radio-telescope aperture. The system temperature $T_{sys}$ varied in the range 150–200 K, depending on the weather. The flux calibration was carried out using observations of DR21, Vir-A, and Cyg-A. The width of the 22-GHz antenna beam was 150″. The sensitivity of the radio telescope was 13 Jy/K.

It was possible to receive the data in either circular or linear polarizations. In the latter case, a polarizer whose operation was based on the Faraday effect was used. The polarizer was operated in an automated regime. The digital output signal from the radiometer was integrated for three minutes for each rotation of the polarization plane of the polarizer by a specified angle, and recorded using the spectrum analyzer. The antenna temperature of the received radiation was calibrated using the signal from a noise generator. The temperature of the calibration step of the noise

generator was established using a known temperature difference at the telescope aperture, provided by matched loads at the aperture, located at room temperature and the temperature of liquid nitrogen.

The receiver system operating at 1.35 cm was mounted at the secondary focus of the 22-m radio telescope. Adjustable heterodynes synchronized with a high-stability 5 MHz signal from a VCH-1005 hydrogen frequency standard were used to transform the input receiver frequencies into intermediate frequencies with a bandwidth of 4 MHz [21]. The cycle used for the maser observations consisted of 5–10 min integrations of the signal toward the source (ON) and offset from the source direction by 1° (OFF). These cycles could be repeated until the desired signal-to-noise ratio was achieved.

The observations at the Hartebeesthoek 26-m (HartRAO, South Africa) and Torun 32-m (Poland) telescopes were methodically similar to those at the Simeiz telescope. The HartRAO observations were carried out using a cryogenic radiometer operating at 22.2 GHz and a spectrometer with a bandwidth of 8 MHz, corresponding to a velocity resolution of 105 m/s. The digital autocorrelator used at the Torun telescope had 4096 channels and a velocity resolution of about 26 m/s.

## 3. MODEL MASER SOURCE

$H_2O$ emission is believed to arise in denise, gas–dust clouds in compact HII regions. In the case of the known kilomaser W49, a single O5 star could produce the observed IR luminosity and create the existing HII region [22]. The dust concentrated in the HII region is probably in the shape of cocoons formed by the IR radiation from the O5 star [23]. Since $H_2O$ is vaporized at temperatures of $T \approx 100$ K, radiative heating of icy grains leads to the formation of water vapor.

The O5 star, with a luminosity of $L \approx 5 \times 10^5 L_\odot$, can destroy dust particles at distances $R_{\rm HII} \approx 8 \times 10^{17}$ cm, and create a compact HII region [24]. The water masers are pumped by IR radiation from dust, UV radiation from the central star, or collisions [25]. The strong variability of the $H_2O$ lines is most likely related to the short lifetimes of water molecules compared to the time scales for photodissociation processes occuring in the intense UV radiation field [26]. Temperature instabilities in the dust cocoons could even lead to the formation of appreciable dust "clumps" [27]. The disappearance of $H_2O$ features may be due to the depletion of "sources" of water vapor [22]. In this picture, the $H_2O$ masers are localized in a dust layer in a compact HII region that is expanding at the speed of sound, in a first approximation ($v_s \approx 10$ km/s).

It is possible that individual features in the $H_2O$ emission correspond to low-mass protostars [28]. In this case, the velocity dispersion of the lines should correspond to the scatter of the kinetic energies of the individual protostars in the protocluster. The total mass of the cluster corresponding to its gravitational boundary ($R \approx 1$ pc) should then be of order $M_{\rm c} \approx 2 \times 10^3 M_\odot$. Such masses are typical for Galactic open clusters.

Interferometric observations show that the $H_2O$ masers are closely associated with submillimeter and IR sources, confirming the importance of IR radiation in pumping the masers. A dense dust envelope with temperatures $T \approx 40$ K in which the maser clumps are embedded can give rise to absorption in the visible by up to a thousand magnitudes. The optical depth $\tau$ in the IR and in the submillimeter sources is appreciably lower [11]. Providing the maximum energy release in the IR requires that $\tau$ not greatly exceed unity. Apparently, this condition is realized in masers.

Flares cannot be explained by a single ejection of energy that increases the pumping rate and then leads to a flare that then dies off due to diffusion [29]. Most likely, conditions are realized for which a water-vapor cloud is subject to the action of sporadic energetic events that lead to a strong increase in the pumping rates, temperatures, and densities of the maser regions in the cloud. Appreciable growths in intensity—by a factor of several hundred during flares—can be explained by unsaturated masers in which the emission rate is stimulated for some reason [30]. In this case, the maser emission grows exponentially with the pumping rate. The linear polarization reflects the key role of the magnetic field in creating the physical processes leading to saturation of the masers.

For example, the linear polarized flux in Orion KL grows linearly to a million Jy (60%) and then remains constant with increasing flux [30]. At lower fluxes, the degree of polarization increases in proportion to the flux, stimulating the rates of emission and relaxation [31]. Thus, the final result is that saturation of the $H_2O$ maser emission is observed. The unsaturated stage can lead to an increase in the pumping energy by a factor of sevral hundred.

No appreciable variations of the line velocity, 8 km/s, or of features associated with the line were detected for Orion KL [32], which may indicate that this feature flares in an isolated fashion.

## 4. MONITORING OF THE SPECTRAL FLUX DENSITY OF IRAS 18316-0602 IN THE $H_2O$ LINE

IRAS 18316-0602 is not prominent in the IRAS catalog, and initially did not attract much attention.

In contrast, the super-powerful flares that occurred in IRAS 18316-0602 at the end of 2016 and in September 2017 through February 2018 raise the question of how such an ordinary source could increase its flux in the water-vapor line to nearly $1.3 \times 10^5$ Jy, that is, by nearly a factor of 1000.

According to [33], IRAS 18316-0602 is located about 3.3 kpc from the Sun. In this case, it should have a bolometric luminosity $L_{\rm bol} \approx 2.5 \times 10^4 L_\odot$. The bulk of the luminosity of the gas–dust cloud is concentrated in the IR and submillimeter. This comprises a luminosity two orders of magnitude lower than the luminosities of the brightest objects in the IRAS catalog. This modest luminosity implies a spectral type for the exciting star of B0 ($T_{\rm eff} \approx 3 \times 10^4$ K) and a comparatively low density for the gas, $n_{\rm H} \approx 2 \times 10^4$ cm$^{-3}$ [34].

The situation changed considerably after the appearance of measurements of the dynamical distances of a large number of Galactic maser objects [35]. New data on the distance to our source were obtained in 2011 based on an analysis of HI spectra in the directions of methanol masers (6.7 GHz). IRAS 18316-0602 was one of 442 sources selected from a sample of methanol masers. Kinematic distances to these sources were determined using a model for the Galactic rotation curve assuming circular orbits for the objects around the Galactic center. A refined rotational velocity of the Sun around the Galactic center was used, 246 km/s. The resulting kinematic distance to G025.650+1.050 (IRAS 18316-0602) is 12.5 kpc. It is important that this value was determined for a range of radial velocities in the maser source of 40.6–41.9 km/s. The water-vapor lines that flared in IRAS 18316-0602 at the end of 2016 and during September 2017–February 2018 are near this range. According to these data, IRAS 18316-0602 is located beyond the Galactic center, and is one of the most distant masers observed in our Galaxy.

According to this distance to the maser, the bolometric luminosity in the IR is $L_{\rm bol} \approx 5 \times 10^5 L_\odot$. These data indicate that IRAS 18316-0602 is among the brightest IR objects in the Galaxy, together with IRAS 18507+0110 ($L_{\rm bol} \approx 7.5 \times 10^5 L_\odot$), IRAS 18314-0720 ($L_{\rm bol} \approx 1.0 \times 10^6 L_\odot$), and IRAS 18449-0158 ($L_{\rm bol} \approx 1.8 \times 10^6 L_\odot$). The exciting star is classified as O4, with an effective surface temperature of $5.8 \times 10^4$ K. That is, we may be dealing with a massive, hot giant with a mass of tens of solar masses, that is capable of ionizing the dense ambient medium to distances of $10^{17}$–$10^{18}$ cm.

This moves IRAS 18316-0602 from being an unexceptional object to being one of the most powerful Galactic kilomasers, whose power exceeds those of W49N and Orion KL. We took into account the fact that the peak flux density in the water-maser line in a 50 kHz bandwidth during the last double flare in September 2017–February 2018 approached $1.3 \times 10^5$ Jy.

Observations of this source were begun in 2000, but were initially carried out only episodically. No serious flux-density increases were noted. Figure 1 plots the dependence of the flux density in the water line as a function of observing epoch. Most of the data shown in this plot were published in [7, 36] (pluses); our observations are shown by squares. Figure 1 shows that three isolated large flares whose amplitudes grew in time occurred during 2000–2017. Although the maximum of the flare occurring in 2002 was not fully traced, it is clear that it was lower than the next maximum in 2010–2011. The flare at the end of 2016 had the highest amplitude [36].

Together with the increasing amplitudes of these flares, the opposite tendency can be noted for their duration. The duration of the 2002 flare was about two years, that of the 2010–2011 flare about one year, and that of the flare at the end of 2016 about one month. It cannot be ruled out that different objects are responsible for the flares in 2002, 2010–2011, and 2016.

If we interpret the long-term monitoring of the amplitude of the $H_2O$ maser flaring as indicating quasi-period behavior, the corresponding period is $T_{\rm per} \approx 7$–$8$ yrs. However, the amplitudes of the superflares used to define this period vary over an order of magnitude, growing with time. It is not simple to identify a physical process occurring on a time scale of 15 years (the time between the first and third superflares) that could explain this time dependence of the amplitude:

$$\log(A_2/A_1) \approx k \log \Delta T, \qquad (1)$$

where $A_2/A_1$ is the ratio of the amplitudes of a flare and the preceding flare, $\Delta T$ the time between the flares in years, and $k \approx 0.5$ is a constant.

Quasi-harmonic variations of the water-maser amplitude on time scales of about 10 years were noted in G59.78+0.06, Sh2-128, and Sh2-184 in [37]. A possible superperiod of 15–16 yrs in W Hydrae was noted by Rudnitskii et al. [38], who suggested this period was related to variations in the activity of the central star.

After the last water-maser flare in IRAS 18316-0602 in September 2017, our monitoring was usually carried out daily (Fig. 2) [39, 40]. The variations of the spectral flux density show two peaks. This shape may indicate the presence of sharp variations in the physical characteristics of the regions of water-vapor emission, possibly related to sudden increases in energy. The shape of the flux-density variations

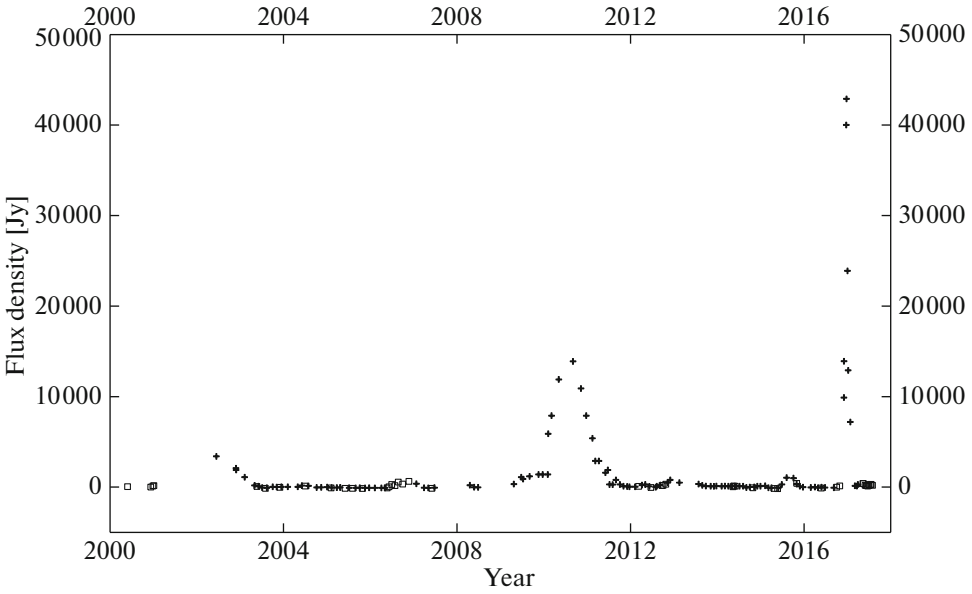


**Fig. 1.** Long-term monitoring of IRAS 18316-0602 in the water line.

(exponential growth and fall-off of the flux, and its two-peaked form) rules out the possibility that the flaring was associated with beaming of the emission. Therefore, this is also unlikely as an explanation for the water-maser flux-density variability.

Another distinguishing feature of the last giant flare in IRAS 18316-0602 is its duration, which is appreciably shorter than those of the first two flares (Fig. 1). The total duration of the double flare in 2017–2018 and the flare at the end of 2016 (15 months) is comparable to the duration of the 2010–2011 flare. If the source of the flares is the same, this could be related to the fact that the amount of data for the first two superflares is quite low. The 2010–2011 flare is represented by seven points, and the 2002 flare by only three points. With this sparseness of the observations, with data being taken at intervals of two to three months, we could get the visual impression that we are dealing with several merging flares, when the maser-deactivation processes gave way to maser-activization processes between observing epochs (Fig. 1). It is not ruled out that powerful water-maser flares in IRAS 18316-0602 occurred with growing ampltude starting from 2002 in accordance with (1), activating various sources.

The giant water-maser flare in G25.65+1.05 (IRAS 18316-0602) in September 2017–February 2018 was the fourth most powerful flare over the history of observations of this source. Detailed flux-density monitoring during a flare can make it possible to draw important conclusions related to the shape of the flare.

The flares are not symmetrical. The rises and falls in the double flare indicate that they can be approximated by exponential dependences (Fig. 2). The exponential shape of the maser flux-density curve serves as an important indicator of the state of the maser during the flare: it is operating in an unsaturated regime, when the maser amplification grows exponentially with the pumping rate [30].

The shape of the central part of the maser line near the maximum phase (decreasing to 50 kHz) testifies that one component in the source is responsible for most of the flux-density increase. Examples of recordings of the IRAS 18316-0602 water-vapor line near the maxima of the first and second flares in 2017–2018 are shown in Figs. 3 and 4.

Analyzing the rises and falls of the flares below 20 000 Jy, it becomes obvious that the object emitting the water line does not have only one component; it probably has at least two components, one of which is less strongly activated. Examples of recordings of the line during flares up to 20 kJy are presented in Figs. 5 and 6.

A second component of the flare with a bell-like shape is clearly visible in Fig. 2 (scaled, like all subsequent figures, to the maximum flux density in the line). The total duration of this component is four months. It began at the start of September 2017, and was present until the end of 2017. The amplitude of this component of the flare (20 kJy) exceeded the amplitude of the flares in 2002 and 2010–2011, in accordance with (1). We therefore conclude that the source giving rise to the bell-like flare in IRAS 18316-0602 in 2017–2018 is the same as the source giving rise to the flares in 2002 and 2010–2011, but with a

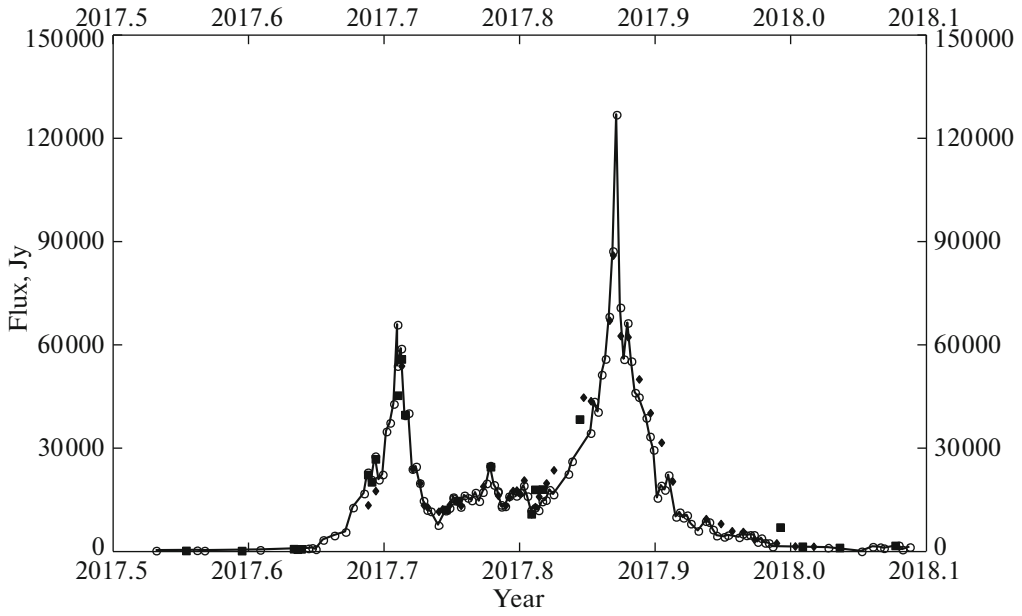


**Fig. 2.** Double flare of the maser emission from IRAS 18316-0602. The circles, squares, and diamonds show the data for the Simeiz, Hartebeesthoek, and Torun radio telescopes, respectively.

flare amplitude (20 kJy) that is a factor of 1.5 higher than the 2010–2011 flare.

It is also clear that, like the flare at the end of 2016, the narrow, double exponential maser flare of 2017–2018 has a different origin than the 2002 and 2010–2011 flare. This is clearly visible in our double flare, which encompasses both sources associated with all previous flares. Another distinguishing feature of the 2017–2018 flare is its double nature.

As in the case of the 2016 flare [36], a dependence of the line width on the flare amplitude is observed for the 2017–2018 flare.

Figure 7 presents this dependence in a plot of $\Delta V^{-2}$ versus $\ln F$, where $F$ is the flux density at the maximum in Jy and $\Delta V$ the line width at the half-maximum level in km/s. The measurements are shown as points, which have been fitted by the straight line shown. The line is strictly symmetrical and very well described by a Gaussian at the activity maximum. This also shows that the maser is in an unsaturated state. However, the data do not exhibit a clearly pronounced character. Similar results were also obtained for the giant flare in Orion KL [41, 42], where it was concluded that the maser was in an unsaturated state nearly up to the maximum amplitude of the flare.

Note also that the radial velocities of the maser lines for the two flare components in 2017–2018 are essentially the same, near 42.8 km/s. This means that the emission zones should be located near each other. Nearby maser clumps should radiate the maser line at similar radial velocities, but the characteristics of the amplitude variations can differ. It is not very clear how a single external pumping source could operate in such different ways. It may be that the answer is related to differences in the characteristics of the maser clumps, whose radiation gives rise to different flare amplitudes and durations.

The giant flare amplitude (about 130 kJy) and distance to the source (12.5 kpc) make IRAS 18316-0602 the most powerful kilomaser in our Galaxy. As in the case of W49, if the primary energy source giving rise to the observed IR luminosity is a single star, it must have a spectral type of at least O5, and possibly O4. This is one of the most massive stars in the Galaxy.

## 5. LINEAR POLARIZATION MEASUREMENTS FOR IRAS 18316-0602

The linear polarization of IRAS 18316-0602 in the water line was measured on September 17, 2017, at the phase of the first maximum of the double flare, using the observing methods described in Section 2. For each rotation of the polarizer polarization plane by a specified angle, the output signal of the radiometer was integrated over 3 min using the spectrum analyzer. Since these observations were carried out at the meridian, the position angle for the maximum amplitude corresponds to the position angle of the linear polarization of the source, equal to −22°.

The degree of linear polarization was calculated using the formula

$$P\% = (P_{\max} - P_{\min})/(P_{\max} + P_{\min}), \qquad (2)$$

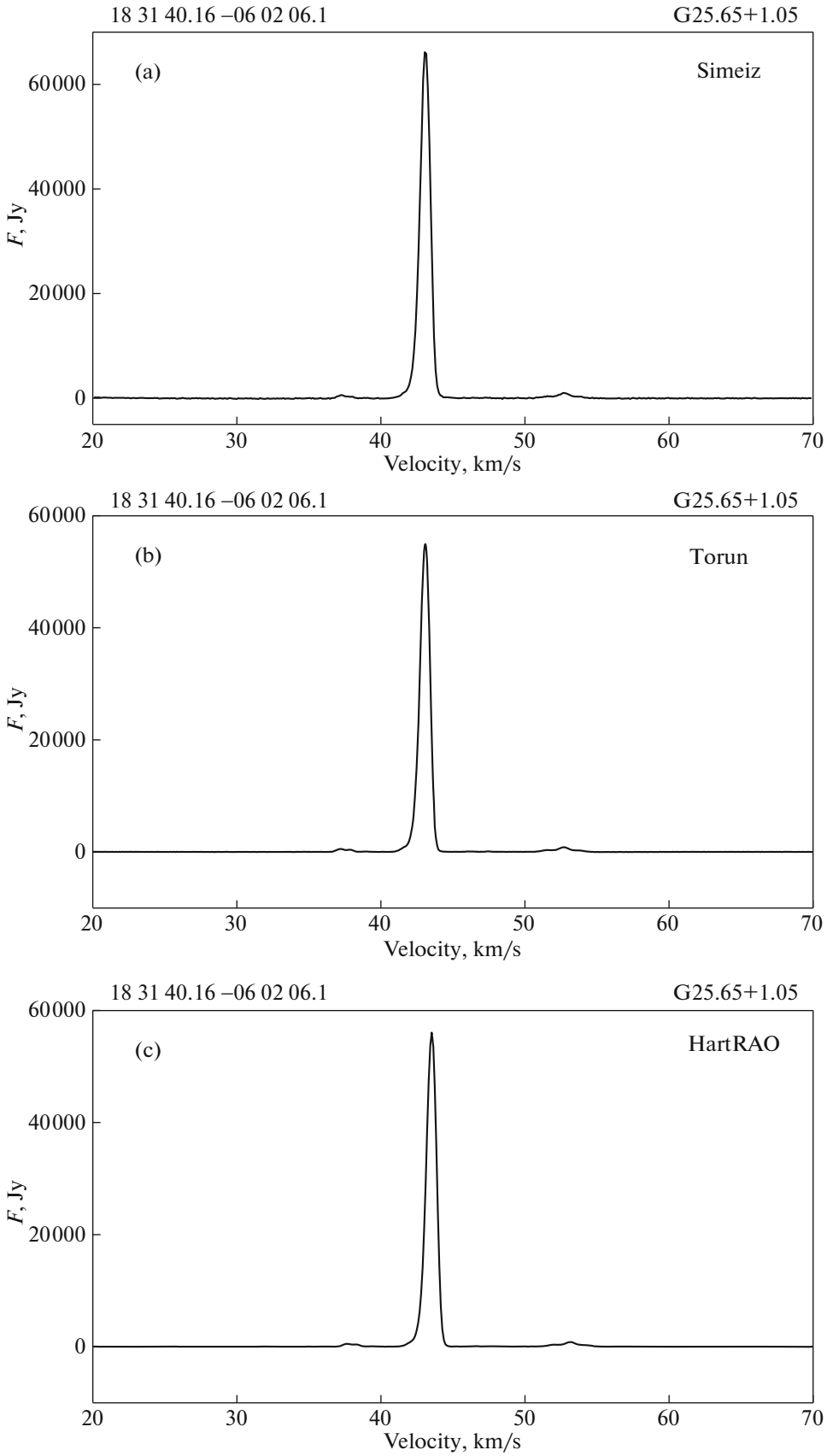


**Fig. 3.** Example of a recording of the water line in G25.65+1.05 (IRAS 18316-0602) at the maximum of the first flare of 2017–2018.

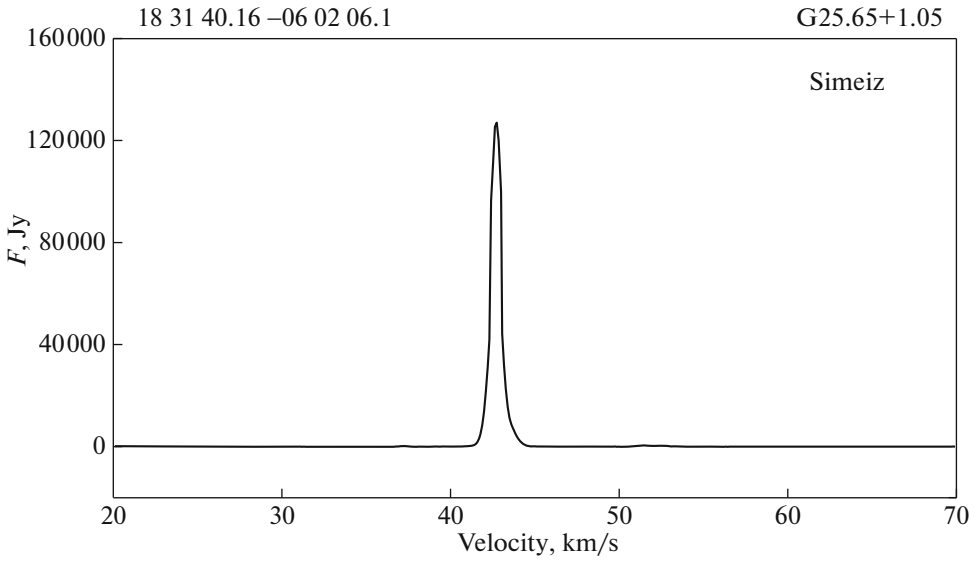


**Fig. 4.** Example of a recording of the water line in G25.65+1.05 (IRAS 18316-0602) at the maximum of the second flare of 2017–2018.

where $P_{max}$ is the maximum and $P_{min}$ the minimum linearly polarized flux density.

The maximum degree of linear polarization was about 30%, which is nearly half the maximum degree of linear polarization during powerful flares in other known kilomasers such as W49 and Orion KL. For example, the degree of linear polarization in a giant water-maser flare in Orion KL in 1980 reached nearly 60% [43, 44]. The linear growth in the polarization with the flux density in the $H_2O$ maser as it increased by more than a factor of 100 during this 1980 flare is an indication that the maser was unsaturated, with the stimulation of the emission rate dominating and the maser amplification growing exponentially with the pumping rate [30]. The degree of polarization remained constant as the fux density in the flare of 1980 grew from $10^6$ Jy to its maximum value of $2.2 \times 10^6$ Jy. In this case, the maser amplification grew linearly with the pumping rate and the maser became satured.

Since the degree of linear polarization in the 2017–2018 flare of IRAS 18316-0602 was about a factor of two lower than in the 1980 superflare in Orion KL, it is natural to propose that the maser source in IRAS 18316-0602 was in an unsaturated state during this flare. This provides additional support for an unsaturated state for the water maser in IRAS 18316-0602, in addition to the exponential form of the flux-density variations.

Further evidence for an unsaturated state of the maser amplification is given by the behavior of the width of the water maser line. According to the model for maser-line profiles proposed in [45], in the case of an unsaturated maser, the line width decreases with increasing flux density as

$$\log P = A + B\Delta\nu^{-2}, \quad (3)$$

where $P_{max}$ is the flare flux density and $\Delta\nu$ is the width of the water maser line during the flare. The observational data are consistent with this picture, but the available accuracy hinders unambiguous conclusions.

Thus, we had the main conditions for the existence of an unsaturated maser during the double water-maser hyperflare in IRAS 18316-0602 in 2017–2018. An exponential growth of the flux density was observed in the growth phase. This is true for both the first and the second flares. This is followed by an exponential decrease in the flux, also in both flares. A moderate degree of linear polarization was measured at the flux-density maximum of the flare.

## 6. INTERFEROMETRIC OBSERVATIONS

The interferometric structure of the water masers can be derived from ground and ground–space VLBI observations. We had no such data at our disposal for IRAS 18316-0602 before the 2017–2018 flare. Considering the structure and physical characteristics of the region in which the flaring $H_2O$ maser in the Orion KL kilomaser was located, we can assert that both the kilomaser itself and the central region of the IR source IRc5 are located in a compact region with a size of about one arcsecond (about 500 AU). The submillimeter source C29 is also nearby [46]. The radio source identified with this object has been mapped with the VLA [47]. A large number of other molecular lines are located in this same region. The

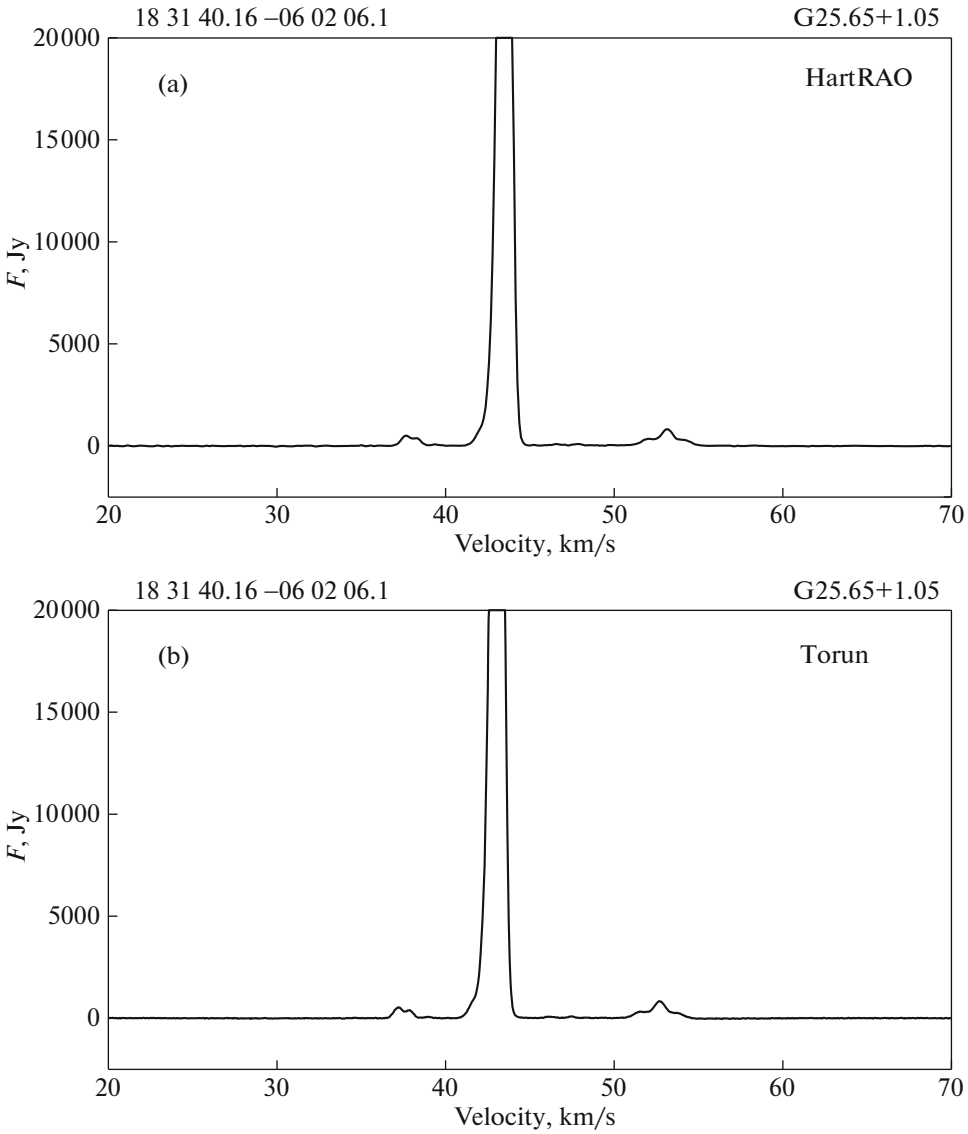


**Fig. 5.** Example of a recording of the water line in G25.65+1.05 (IRAS 18316-0602) at the maximum of the first flare of 2017–2018, to the 20 kJy level.

gas–dust cloud radiating as an IR source serves as a source of pumping for the $H_2O$ maser, which is heated by shocks propagating from the outer source [48]. This source must be an early-type star.

The size of the $H_2O$ maser spot in Orion KL is $0.95 \times 0.40$ AU. The peak flux was about $10^6$ Jy, indicating a brightness temperature of $1.2 \times 10^{14}$ K. The isotropic luminosity is $L = 2.4 \times 10^{-4} L_\odot$ for a line width of 0.6 km/s [49].

Why is it in such regions that the $H_2O$ maser flares, and in lines that have velocities close to the mean velocity of the bulk of the gas where the maser is located? Specific, and possibly configurational, conditions for the maser pumping must be created in the region where the maser is located. Such conditions arise where the velocity is not very different from the mean velocity of the molecular cloud [50]. One of the most important conditions for a maser flare could be an interaction of a maser clump and a bipolar ejection from a young protostar [51].

The location of the maser relative to the center of the submillimeter cloud is important. ALMA data with a resolution of 0.3″ (≈160 AU) show that the supermaser is located within the submillimeter core, no farther than 160 AU from its center [50].

Based on an analysis of their structure and proper motions, the maser clumps were located along a Northwest–Southeast line during the flare in Orion KL, perpendicular to the low-velocity outflows in the source [52].

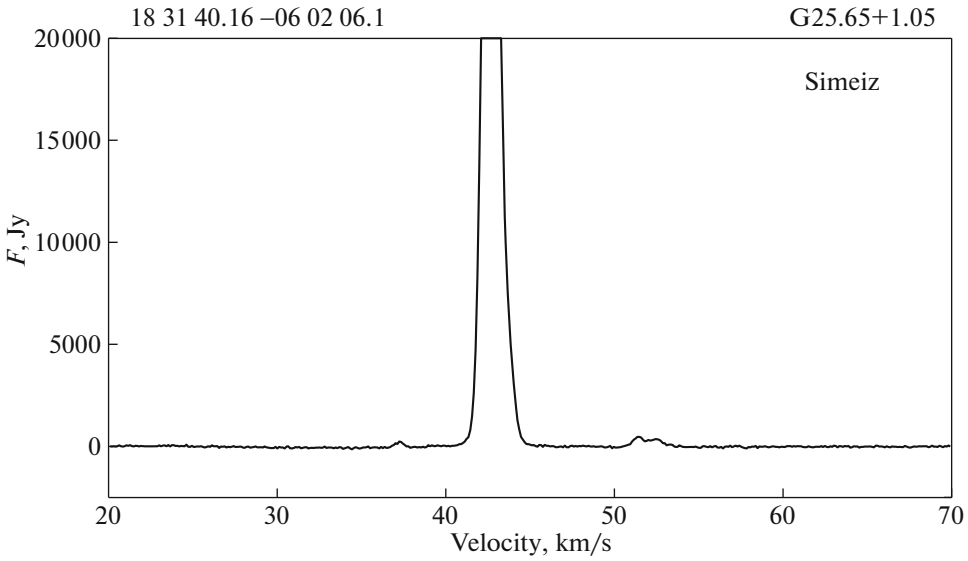


**Fig. 6.** Example of a recording of the water line in G25.65+1.05 (IRAS 18316-0602) at the maximum of the second flare of 2017–2018, to the 20 kJy level.

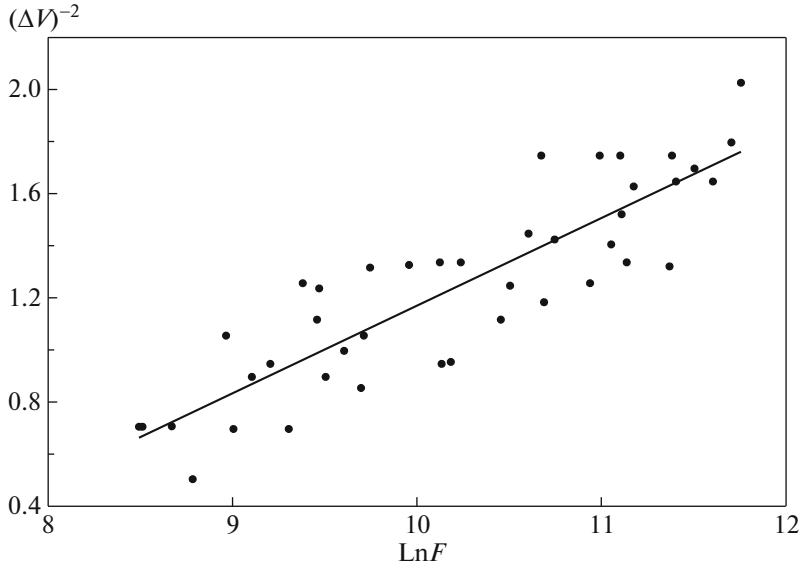


**Fig. 7.** Dependence of the width of the water-maser line on the flux during the flare in G25.65+1.05 (IRAS 18316-0602) in September 2017—February 2018.

The size of the maser spot at the Orion KL flare maximum in 2012 was $2.26 \times 0.95$ mas, which corresponds to a linear size of about 0.4 AU. This indicates that the water-maser clumps must be less than an AU in size. The corresponding brightness temperature and luminosity are $T_{\rm br} = 1.2 \times 10^{14}$ K and $L = 2.4 \times 10^{-4} L_{\odot}$. The dimensions of the water-maser clumps in Orion KL during the 1998 superflare measured with VLBI are less than 0.1 AU. The described conditions should probably be similar in all Galactic kilomasers, including IRAS 18316-0602.

Interferometric observations of IRAS 18316-0602 were carried out in September 2017 in a series of six daily sessions on an interferometer formed by the three 32-m radio telescopes of the "Kvazar" VLBI complex and the 22-m radio telescope in Simeiz. The beginning of the VLBI bandwidth was set to be 22.229 MHz and the duration of each scan of the source was 20 min. The calibrator was 3C454.3, for which scans of 5 or 20 min were observed at the beginning, middle, and end of the session. The data were correlated using the DiFX 2.4.1 software cor-

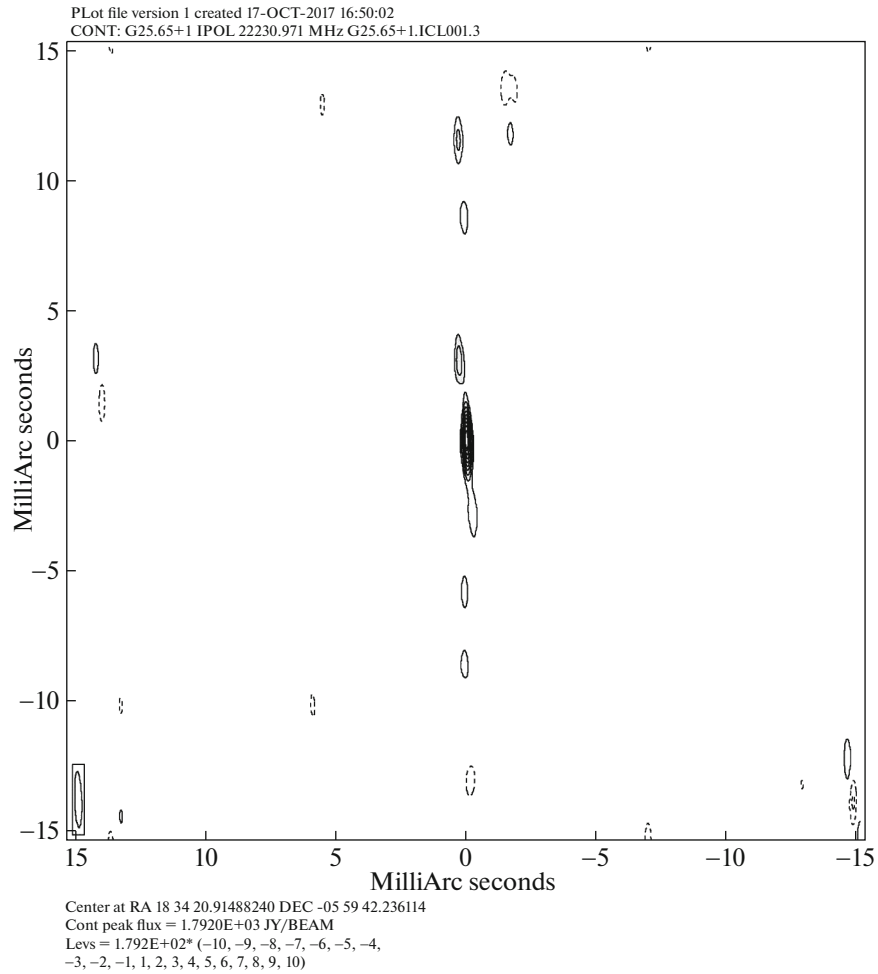


**Fig. 8.** Interferometric image of IRAS 18316-0602 obtained on the Kvazar–Simeiz baseline on September 27, 2017.

relator of the Institute of Applied Astronomy running on a hybrid blade-server cluster. Figure 8 presents an image obtained for September 27, 2017, when the source was in the phase after the first of the two flux-density maxima.

On this map, 1 mas corresponds to a linear scale of about 20 AU, based on a distance to the source of 12.5 kpc. It is difficult to distinguish individual clumps with this resolution, but the overall pattern of the distribution of the emission in this region can be traced fairly clearly. A bright central features can be seen, which it is natural to relate to the clump (or compact condensations) in which the uniquely powerful water-maser flare occurred. All the remaining features have much lower amplitudes.

The resolution realized in these observations is insufficient to distinguish two components of the emission associated with the two flares with their different shapes: one of which corresponds to the central feature in Fig. 2, and the other to a bell-like shape with a lower amplitude. Nevertheless, the interferometric data confirm our earlier conclusions that the different clumps responsible for the different parts of the flare are close to each other and located in a compact region. The data obtained are consistent with the results of observations of other strong Galactic masers, whose compact HII regions have sizes of $l_{\rm HII} \approx 10^{16}$ cm [56]. Consequently, the molecular disks where the maser clumps could be located have sizes of order $l_{\rm disk} \approx 10^{17}$ cm ($\approx 10^4$ AU) or more.

We conclude that these interferometric data obtained during the water-maser flare in IRAS 18316-0602 confirm the presence of the compact clumps responsible for the powerful rise in the flux density during the flare.

## 7. SUBMILLIMETER DATA OBTAINED IN COORDINATION WITH WATER-MASER OBSERVATIONS OF IRAS 18316-0602

Observations of G25.65+1.05 (IRAS 18316-0602) were carried out at 870 $\mu$m near the maximum of the first water-maser flare on September 15–16,

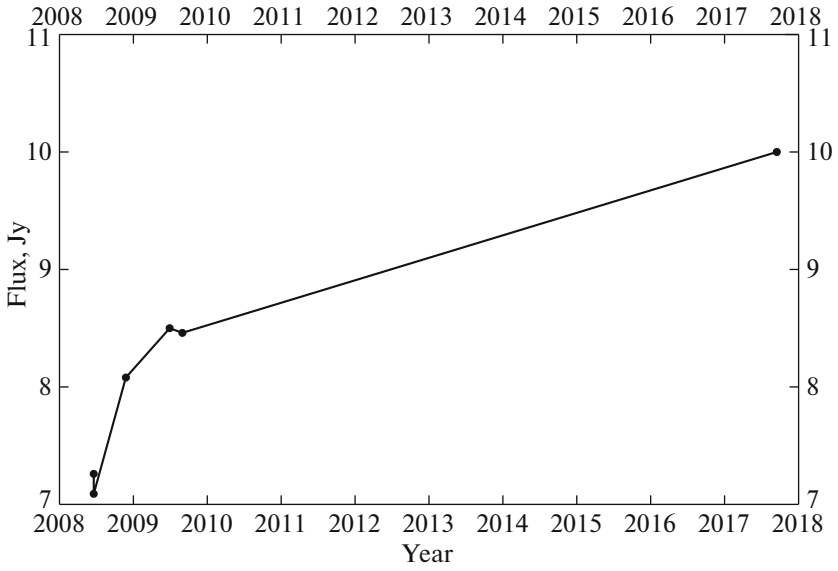


**Fig. 9.** Long-term flux-density variations in G25.65+1.05 (IRAS 18316-0602) at 870 $\mu$m, obtained on the APEX large bolometric camera.

2017 under favorable observing conditions on the APEX large bolometric camera (LABOCA, [57]).

The focus of the telescope was optimized using observations of the planet Saturn, and pointing corrections were determed using observations of the nearby point source J1743-038. Saturn, the hot molecular cloud G34.26+0.15, and G10.62-0.38 were used as calibrators. Two of these Galactic sources were observed on the two days before and after the observations of G25.65+1.05.

The long-term variations of the flux density of G25.65+1.05 at 870 $\mu$m are shown in Fig. 9. Over the interval from 2008 through 2018, the spectral flux density grew by 40%, from 7 Jy to 10 Jy. Half of this rise occured at the onset of the 2010 flare (to 8.5 Jy), while the second half (to 19 Jy) occurred during the first (double) flare of 2017 (September 15–16, 2017).

The submillimeter flux, which is a continuation of the IR emission, varied by tens of percent during the water-maser flares. This may provide evidence that the primary source of activity could be a central massive star that is hidden from view by gigantic absorption in the optical, possibly by up to hundreds of magnitudes.

It is important to determine whether the rise in the submillimeter flux preceded the onset of the water-maser flares. The plot in Fig. 9 suggests that this is the case. By the beginning of 2010, the submillimeter flux had already risen to 8.5 Jy, and reached a local maximum of sorts. The water-maser flare began from this time on during 2010–2011. Unfortunately, the submillimeter data are then absent until September 2017, when the most powerful flare occurred, with the submillimeter flux being 10 Jy at the flare maximum. Thus, we conclude that rises in the submillimeter flux, and possibly also the IR flux, are related to maser flares, accompanying or even preceding these flares.

Figure 10 shows a map of G25.65+1.05 (IRAS 18316-0602) obtained with the APEX large bolometric camera in September 2017 during the maser flare. Figure 11 shows a map of this source obtained as a fragment of the ATLASGAL catalog. The resolution of this map is indicated by a red circle in the lower left corner of the figure. The size and orientation of the source are indicated by the blue ellipse. The green ellipse marks the location of several sources found in a Galactic plane survey. The image size is $5' \times 5'$. The coordinate accuracy in the catalog is not sufficient to enable a comparison of the source coordinates with the interferometric positions. The coordinates are coincident to within a few arcseconds. This corresponds to tens of thousand of AU, taking into account the distance to G25.65+1.05 (IRAS 18316-0602).

Figure 12 presents an image of G25.65+1.05 (IRAS 18316-0602) obtained in the middle section of the IR band using the IRAC band filters (3.6 $\mu$m, 4.5 $\mu$m, 5.8 $\mu$m, 8.0 $\mu$m). These data were taken from the GLIMPSE Legacy Project. The image resolution is shown by the red circle in the lower left corner. The source is located at the center of the map. The coordinates of the submillimeter and IR sources coincide within the uncertainties, consistent with the physical conditions that are realized in young Galactic objects.

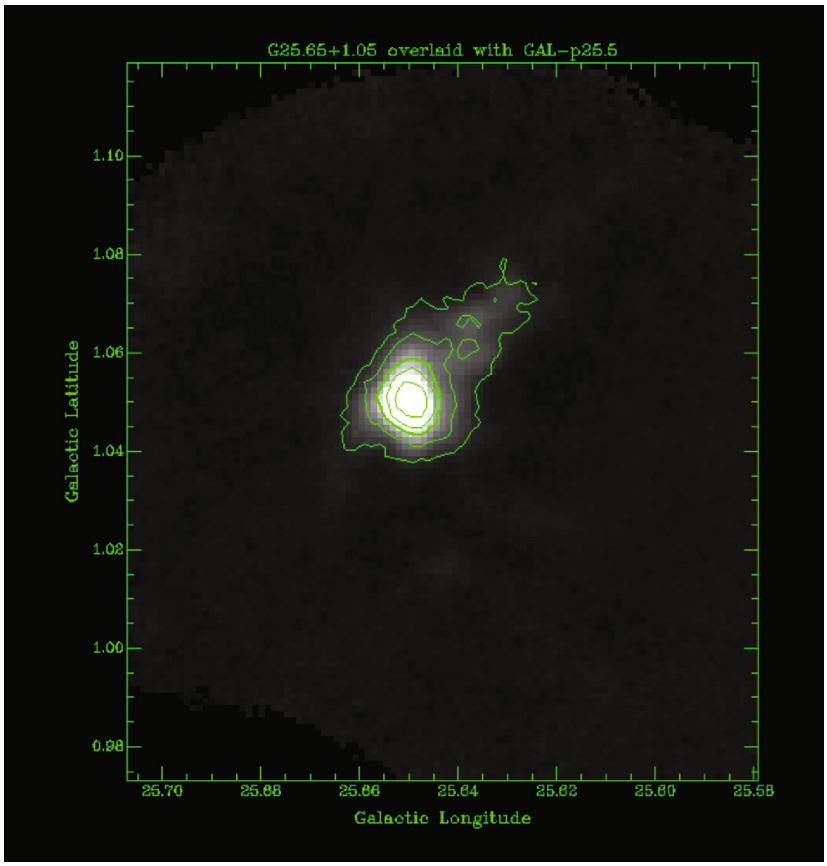


**Fig. 10.** (Color online) Image of G25.65+1.05 (IRAS 18316-0602) obtained at 870 $\mu$m with the APEX large bolometric camera.

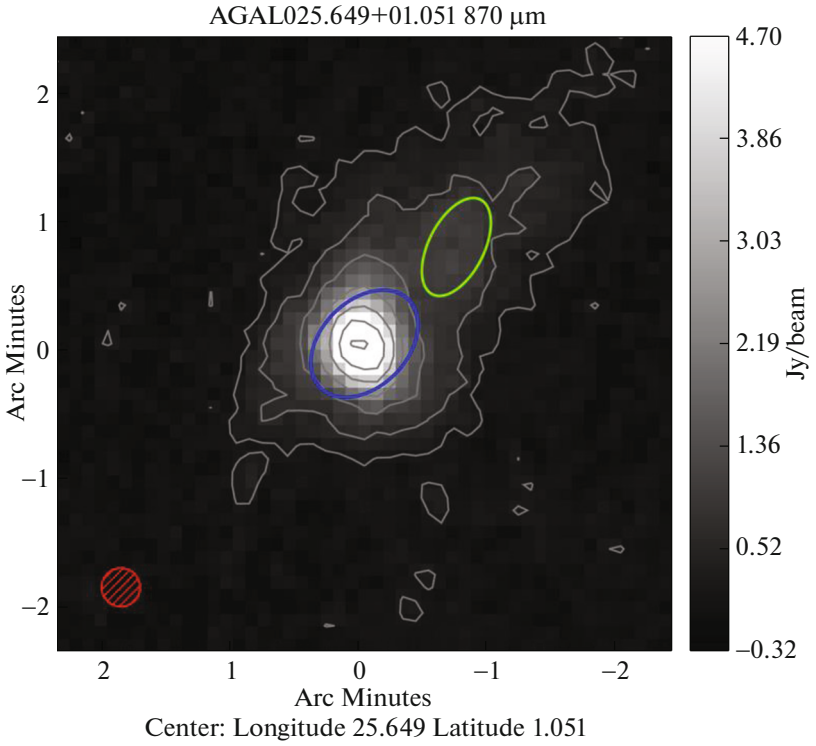


**Fig. 11.** (Color online) Image of G25.65+1.05 (IRAS 18316-0602) from the ATLASGAL catalog.

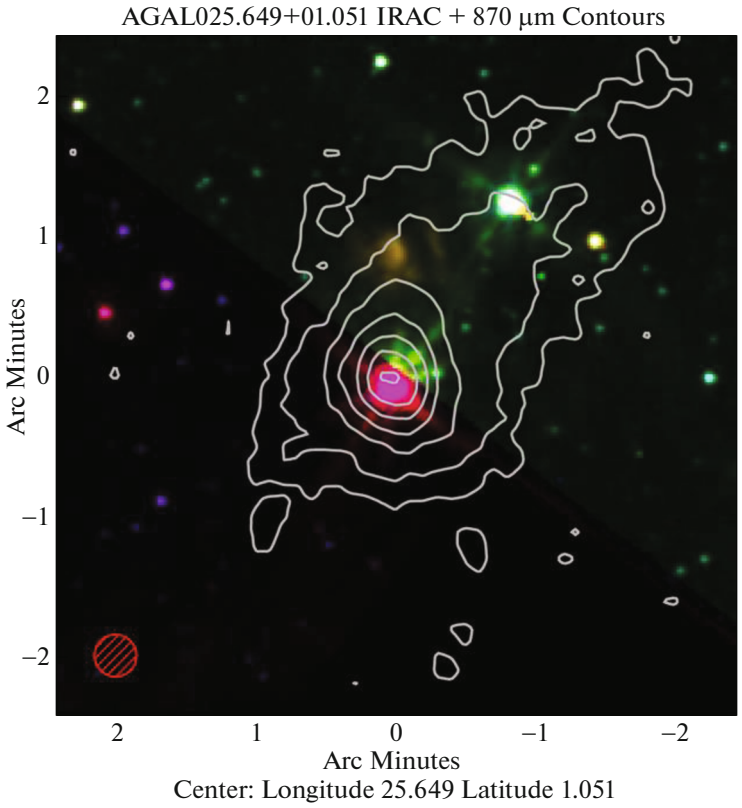


**Fig. 12.** (Color online) Image of G25.65+1.05 (IRAS 18316-0602) in the mid-IR (3.6 $\mu$m, 4.5 $\mu$m, 5.8 $\mu$m, 8.0 $\mu$m).

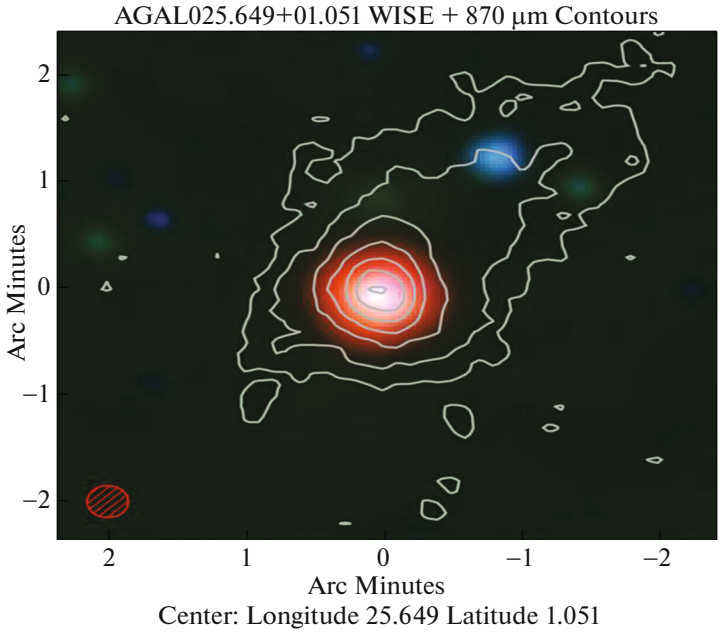


**Fig. 13.** (Color online) Image of G25.65+1.05 (IRAS 18316-0602) in the mid-IR (3.4 $\mu$m, 4.6 $\mu$m, 12 $\mu$m, 22 $\mu$m).

Figure 13 shows an image of G25.65+1.05 (IRAS 18316-0602) in the middle section of the IR band using the WISE band filters (3.4 $\mu$m, 4.6 $\mu$m, 12 $\mu$m, 22 $\mu$m). The image resolution is shown by the red circle in the lower left corner. The source is located at the center of the map. The two IR maps in Figs. 12 and 13 correspond to each other well.

## 8. SOURCES OF PRIMARY ENERGY RELEASE IN THE IRAS 18316-0602 SYSTEM

This section has a speculative character.

Giant water-maser flares should be associated with powerful sources of primary energy release that lead to an increase in the flux density in the water line by two orders of magnitude or more. Such sources include the IR radiation of the molecular gas–dust cloud in which the maser clumps are embedded and/or systems of powerful shocks propagating from the central stellar object. Maser lines can also be excited by bipolar outflows. In all this, it remains unclear what precisely triggers the activity of the central stellar objects, which may include both late-type T Tauri stars and massive early-type stars that are approaching the main sequence.

A number of hypotheses about the mechanisms triggering the emission in the water line in Galactic sources have been put forth, and are generally related to variations of both the dust temperature and the photon flux density from the central source.

Giant water-maser flares in Galactic kilomasers (Orion KL, W49, IRAS 18316-0602) are rare, and occur no more often than once every 5–10 years. What physical processes initiate these flares, which can be accompanied by line flux densities that grow by a factor of 100? There is no doubt that the main energy release in the system is provided by a massive early-type star located in the pre-main-sequence phase. As a rule, the formation and evolution of such stars is hidden from direct observation due to the gigantic absorption in the optical in the direction toward such stellar complexes. The IR spectrum has a maximum in the far IR, indicating appreciable absorption at these wavelengths. It is possible to observe compact HII regions only in the radio; these testify to the presence of massive early-type stars that ionize the surrounding space out to distances of $10^{18}$ cm from the supermassive central star. Nevertheless, there remains the question of whether a single star or multiple stars ionize this region.

About half the stars in galaxies are in double or multiple systems. These most likely formed during the evoution of gas–dust clouds, through their fragmentation. An important aspect of this is interactions of these multiple systems that could provide possibilities for igniting sources of primary energy release in the gas–dust clouds. How do such sources lead to giant flares in water kilomasers?

The main mechanisms exciting the $H_2O$ masers include radiative and collisional mechanisms. The former comes about due to a transformation of photons from the central star into a source of IR radiation in the nebula, and the latter is due to a system of shocks passing through the medium where the maser clumps are located. The question of the sources of the giant explosive energy release manifest in powerful water-maser flares remains.

The latest double $H_2O$-maser flare in IRAS 18316-0602, when the maser was in an unsaturated state, suggests that the activization of the maser is realized over a month, after which there is an exponential decay in the flux density. What process could lead to such pumping of the $H_2O$ molecules in an isolated maser clump? The presence of a narrow line at a fixed frequency indicates the presence of a single clump. The radiation parameters in the line would seem to indicate a high density, appreciable mass, and a large temperature difference preserved over a substantial period of time of the order of a month. However, it is not simple to identify a physical process that can lead to changes in the characteristics of the maser clump while preserving the unsaturated state of the maser over tens of days, and that ends as suddenly as it began.

The source of primary energy release is unlikely to be a powerful stellar wind due to its comparatively low energy. Accretion is not a very suitable energy source, since the last flares in IRAS 18316-0602 at the end of 2016 and in 2017–2018 had similar durations, and we would not expect such regular accretion.

Models with hot, dense material in a rotating accretion disk [50] or pulsational instabilies in massive stars [53] have also been proposed. In this case, the colliding stellar winds from two stars could be responsible for the proposed periodicity [54].

We indeed see some kind of quasi-regular process in IRAS 18316-0602, in terms of both the flare duration and the interval between flares. The occurrence of flares in 2002–2003, 2010, and at the end of 2016 – (2017–2018) may suggest a quasiperiod for the flare activity of about seven years.

Apart from everything else, there is the possibility of double flares. In additon to the flare in IRAS 18316-0602 in 2017–2018, a double flare was observed in Orion KL in 1979–1980 [55].

In principle, partial multiple ejections of the stellar envelope could provide the required energy for this process. With a speed for the ejected envelope of $v \approx 5 \times 10^7$ cm/s (500 km/s), the envelope will traverse a distance of $1.5 \times 10^{14}$ cm (10 AU) over a month, which substantially exceeds the dimensions of the maser clumps. In order for a maser clump to remain

in the activated state over a month, the size of the ejected envelope must be about 10 AU. If the envelope is smaller, the speed of the ejected envelope must be lower. Note that the velocities of ejected supernova envelopes can reach $v \approx 10^9$ cm/s. Thus, we find this mechanism for activation of the maser improbable.

The above reasoning suggests that the source of quasiperiodic activity could be close, massive multiple stellar systems. One possibility is that these are triple stars. The quasiperiod is then determined by the time scale for stability of the systems, on which the third body and the accretion disk disrupt the harmonic condition, and thereby the stability of the flare period.

We can estimate the parameters of the orbit of the components of the proposed system required to obtain the observed characteristics of the water-maser flares in IRAS 18316-0602. Application of the laws of celestial mechanics indicates that, for a central star with a mass of $30M_\odot$ in a binary with a less massive object in an elliptical orbit with semi-axis 25 AU, the period of rotation about their common center of mass would be about eight years. This is close to the quasiperiod between the water-maser supeflares observed in IRAS 18316-0602. Powerful gravitational perturbations of the envelope of the supermassive star arise at periastron, leading to its partial ejection.

When the ejected envelope reaches the accretion disk, where the maser clumps are located, this creates a powerful system of shocks, leading to an explosive increase in the temperature and density in the maser clumps. This also leads to an exponential growth in the pumping of the maser during the entire time covered by the passage of the envelope. After the end of activization of the maser, there is an exponential drop in the flux densty due to the decrease in the density of $H_2O$ vapor, temperature, and matter density in the maser clumps.

It is not yet clear whether the occurrence of double flares is a regular event. If this is confirmed, it will be necessary to identify the physical basis for this phenomenon.

## 9. CONCLUSION

1. We have carried out long-term monitoring of the Galactic kilomaser IRAS 18316-0602 (G25.65+1.05) in the water-vapor line at frequency $f = 22.235$ GHz ($6_{16}$–$5_{23}$ transition) using the 22-m CrAO telescope, 26-m Hartebeesthoek telescope, and 26-m Torun telescope.

2. Our monitoring of this object has enabled us to determine the detailed shape of the flux-density variations during a unique double flare that occurred from September 2017 through February 2018.

3. The exponential rise in the flux density during the first and second parts of the double flare enables us to firmly conclude that the kilomaser was in the unsaturated regime during this flare, right to the flare maximum. Additional evidence for this is provided by the moderate degree of linear polarization (≈30%), lower than the value in the Orion KL Galactic kilomaser.

4. The line shape during the flare testifies that the flare occurred in an isolated source at a frequency close to that of the previous powerful flares in 2002, 2010, and 2016.

5. The 2017–2018 flare revealed the presence of two close sources of maser radiation in IRAS 18316-0602, with different radiation characteristics in the water line. The weaker of these could be responsible for the flares in 2002 and 2010–2011.

6. We have proposed an interpretation for the source of primary energy release in the system that can lead to kilomaser flares and increase the system's flux by more than a factor of 100.

## ACKNOWLEDGMENTS

This work has been supported by the National Science Center of Poland (grant 2016/21/B/ST9/01455). This work was partially supported by Program no. 28 of the Russian Academy of Sciences, "The Cosmos: Fundamental Processes and Their Interconnections", and the Russian Foundation for Basic Research (grant no. 18-42-910018).

## REFERENCES

1. A. C. Cheung, D. M. Rank, C. H. Townes, D. D. Thornton, and W. J. Welch, Nature (London, U.K.) **221**, 626 (1969).
2. B. F. Burke, K. J. Johnston, V. A. Efanov, B. G. Clark, et al., Sov. Astron. **16**, 379 (1972).
3. M. Harwit, D. A. Neufeld, G. J. Melnik, and M. J. Kaufman, Astrophys. J. Lett. **497**, L105 (1998).
4. C. Ceccarelli, E. Caux, G. J. White, S. Molinari, et al., Astron. Astrophys. **331**, 372 (1998).
5. B. Nisini, M. Benedettini, T. Giannini, E. Caux, et al., Astron. Astrophys. **350**, 529 (1999).
6. S. Maret, C. Caccarelli, E. Caux, A. G. G. M. Tielens, and A. Castels, Astron. Astrophys. **395**, 573 (2002).
7. F. Palla, J. Brand, R. Casaroni, G. Comoretto, and M. Felli, Astron. Astrophys. **246**, 249 (1991).
8. S. Kurtz, E. Curchwell, and D. O. S. Wood, Astrophys. J. Suppl. **91**, 659 (1994).
9. W. H. McCutcheon, P. E. Dewdney, R. Purton, and T. Sato, Astron. J. **101**, 1435 (1991).
10. S. Kurtz and P. Hofner, Astron. J. **130**, 711 (2005).
11. T. Jenness, P. F. Scott, and R. Padman, Mon. Not. R. Astron. Soc. **276**, 1024 (1995).
12. W. H. McCutcheon, T. Sato, C. R. Purton, H. E. Matthews, and P. E. Dewfney, Astron. J. **110**, 1762 (1995).
13. L. Bronfman, L. A. Nyman, and J. May, Astron. Astrophys. Suppl. **115**, 81 (1996).

14. S. Molinari, J. Brand, R. Cesaroni, and F. Palla, Astron. Astrophys. **308**, 573 (1996).
15. S. P. Todd and S. K. Ronsay Howat, Mon. Not. R. Astron. Soc. **367**, 238 (2006).
16. E. L. Gibb, D. C. Whittet, A. C. A. Boogert, and A. G. G. M. Tielens, Astrophys. J. Suppl. **151**, 35 (2004).
17. J. Brand, R. Cesaroni, P. Caselli, M. Catarzi, et al., Astron. Astrophys. Suppl. **103**, 541 (1994).
18. D. J. van der Walt, M. J. Gaylard, and G. C. Macleod, Astron. Astrophys. Suppl. **110**, 81 (1995).
19. C. Codella, M. Felli, and V. Natale, Astron. Astrophys. **311**, 971 (1996).
20. N. S. Nesterov, A. E. Vol'vach, I. D. Strepka, V. M. Shul'ga, V. I. Lebed', and A. M. Pilipenko, Radiofiz. Radioastron. **5**, 320 (2000).
21. A. E. Vol'vach, L. N. Vol'vach, I. D. Strepka, A. V. Antyufeev, V. V. Myshenko, S. Yu. Zubrin, V. M. Shul'ga, et al., Izv. Krymsk. Astrofiz. Obs. **104**, 72 (2009).
22. T. M. Heckman and W. T. Sullivan, Astrophys. Lett. **17**, 105 (1976).
23. F. D. Kahn, Astron. Astrophys. **37**, 149 (1974).
24. W. K. Hartmann, Astrophys. J. Lett. **149**, L87 (1967).
25. P. Goldreich and J. Kwan, Astrophys. J. **191**, 93 (1974).
26. I. J. Stief, B. Donn, S. Glicker, E. F. Gentien, and J. E. Mentall, Astrophys. J. **171**, 21 (1972).
27. F. D. Kahn, Astron. Astrophys. **37**, 149 (1974).
28. F. O. Clark, D. Buhl, and L. E. Snyder, Astrophys. J. **190**, 545, (1974).
29. B. F. Burke, T. S. Giuffrida, and A. D. Haschick, Astrophys. J. Lett. **226**, L21 (1978).
30. P. Goldreich, D. A. Keeley, and J. J. Kwan, Astrophys. J. **179**, 111 (1973).
31. P. Goldreich, D. A. Keeley, and J. J. Kwan, Astrophys. J. **182**, 55 (1973).
32. N. L. Cohen and S. H. Zisk, Bull. Am. Astron. Soc. **12**, 507 (1980).
33. S. J. Chan, T. Henning, and K. Schreyer, Astrophys. J. Suppl. **115**, 285 (1996).
34. B. Mookerjea and S. K. Ghosh, J. Astrophys. Astron. **20**, 1 (1999).
35. J. A. Green and N. M. McClure-Griffiths, Mon. Not. R. Astron. Soc. **417**, 2500 (2011).
36. E. E. Lekht, M. I. Pashchenko, G. M. Rudnitskii, and A. M. Tolmachev, Astron. Rep. **62**, 213 (2018).
37. R. Valdettaro, F. Palla, J. Brand, R. Cesaroni, G. Comoretto, M. Felli, and F. Palagi, Astron. Astrophys. **383**, 244 (2002).
38. G. M. Rudnitskii, E. E. Lekht, and I. I. Berulis, Astron. Lett. **25**, 398 (1999).
39. A. E. Volvach, L. N. Volvach, M. Gordon, E. E. Lekht, G. M. Rudnitskij, and A. M. Tolmachev, Astron. Telegram, No. 10728, 1 (2017).
40. L. N. Volvach, A. E. Volvach, M. G. Larionov, G. C. MacLeod, S. P. van den Heever, P. Wolak, M. Olech, Monthly Not. Roy. Astron. Soc. **482**, Issue 1, L90 (2019).
41. T. Omodaka, T. Maeda, M. Miyoshi, A. Okudaira, et al., Publ. Astron. Soc. Jpn. **51**, 333 (1999).
42. T. Shimoikura, H. Kobayashi, T. Omodaka, P. J. Diamond, L. I. Matveyenko, and K. Fujisawa, Astrophys. J. **634**, 459 (2005).
43. Z. Abraham, N. L. Cohen, R. Ophel, J. C. Raffaelli, and S. H. Zisk, Astron. Astrophys. **100**, 10 (1981).
44. Z. Abraham, J. W. S. Vilas Boas, and L. F. del Ciampo, Astron. Astrophys. **167**, 311 (1986).
45. P. Goldreich and J. Kwan, Astrophys. J. **190**, 27 (1974).
46. D. N. Friedal and S. L. Widicus Weaver, Astrophys. J. **742**, 64 (2011).
47. M. Felly, E. Churchwell, T. L. Wilson, and G. B. Taylor, Astron. Astrophys. **98**, 137 (1993).
48. S. Okumura, T. Yamashita, and S. Saco, Publ. Astron. Soc. Jpn. **63**, 823 (1999).
49. T. Hirota, M. Tsuboi, and Y. Kurono, Publ. Astron. Soc. Jpn. **66**, 106 (2014).
50. T. Hirota, M. K. Kim, and Y. Kurono, Astrophys. J. Lett. **739**, 59 (2011).
51. G. Garay, J. M. Moran, and A. D. Haschick, Astrophys. J. **338**, 244 (2011).
52. T. Shimoikura, H. Kobayashi, T. Omodaka, P. J. Diamond, L. I. Matveyenko, and K. Fujisawa, Astrophys. J. **634**, 459 (2005).
53. S. Parfenov and A. M. Sobolev, Mon. Not. R. Astron. Soc. **444**, 620 (2014).
54. K. Inayoshi, K. Sugiyama, and T. Hosokawa, Astrophys. J. **773**, 70 (2013).
55. J. P. Maswanganye, M. J. Gaylard, S. Goedhart, D. J. Walt, and R. S. van der Booth, Mon. Not. R. Astron. Soc. **446**, 2730 (2015).
56. R. Genzel, D. Dowens, J. M. Moran, K. J. Johnston, et al., Astron. Astrophys. **78**, 239 (1979).
57. G. Siringo, E. Kreysa, A. Kovács, F. Schuller, et al., Astron. Astrophys. **497**, 945 (2009).

*Translated by D. Gabuzda*